Real-space pseudopotential method for computing the electronic properties of periodic systems

M. M. G. Alemany,[1] Manish Jain,[1] Leeor Kronik,[2] and James R. Chelikowsky[1]
[1]*Department of Chemical Engineering and Materials Science, Minnesota Supercomputing Institute, University of Minnesota, Minneapolis, Minnesota 55455, USA*
[2]*Department of Materials and Interfaces, Weizmann Institute of Science, Rehovoth 76100, Israel*
(Received 7 August 2003; published 12 February 2004)

We present a real-space method for electronic-structure calculations of periodic systems. Our method is based on the self-consistent solution of the Kohn-Sham equations on a uniform three-dimensional grid. A higher-order finite-difference method is combined with *ab initio* pseudopotentials. The kinetic energy operator, the nonlocal term of the ionic pseudopotential, and the Hartree and exchange-correlation potentials are set up directly on the real-space grid. The local contribution to the ionic pseudopotential is initially obtained in reciprocal space and is then transferred to the real-space grid by Fourier transform. Our method enjoys the main advantages of real-space grid techniques over traditional plane-wave representations for density-functional calculations, i.e., improved scaling and easier implementation on parallel computers. We illustrate the method by application to liquid silicon.

DOI: 10.1103/PhysRevB.69.075101 PACS number(s): 61.20.Ja, 71.22.+i, 71.15.Pd

I. INTRODUCTION

Calculating the ionic and electronic structures of materials from first principles remains a formidable task. Although the Hohenberg-Kohn-Sham density-functional theory (DFT) (Refs. 1 and 2) simplifies the problem enormously, the size of systems susceptible to current quantum computation methods is limited. As such, the development of efficient DFT-based methods is crucial for solving large-scale problems in condensed-matter physics.

Plane-wave pseudopotential methods have been widely used for electronic-structure calculations.[3] Pseudopotential theory allows one to focus on the chemically active valence electrons by replacing the strong all-electron atomic potential by a weak pseudopotential which effectively reproduces the effects of the core electrons on the valence states. This approximation significantly reduces the number of eigenpairs to be handled, especially for heavier elements. Moreover, since the core wave functions and the core oscillatory region of the valence wave functions are removed, the use of simple basis functions such as plane waves is straightforward. Representing the electronic wave functions with respect to a plane-wave basis offers a number of advantages, including (i) that the basis does not depend on atomic positions; (ii) that only one parameter, the wavelength of the highest Fourier mode used in the expansion, need be refined to control convergence; and (iii) that matrix-vector multiplication between the Hamiltonian matrix and the trial wave vectors, which is the crucial computational step in modern pseudopotential codes, can be efficiently performed using the fast Fourier transform (FFT), which improves scaling from the ''standard'' N_a^3 to $N_a^2 \ln N_a$ (where N_a is the number of atoms involved in the calculations).

Also, plane waves have both ''physical'' and computational drawbacks. In a plane-wave representation, the boundary conditions must be periodic. If one wants to study a nonperiodic system such as a molecule or a cluster, nontrivial precautions must be taken to reproduce the vacuum accurately, since spurious interactions between replicated images of the system must be avoided. A periodic representation also complicates the study of charged systems: the periodicity makes the system infinitely charged, so that an artificial uniform compensating charge must be inserted (and subtracted) in order to prevent divergence of the total energy. Furthermore, since FFTs involve nonlocal operations, the efficiency of their implementation on parallel computer architectures is diminished by the need for global communications among processors.

During the past decade, there has been increasing interest in developing real-space pseudopotential methods.[4] Such methods have a number of points in their favor. First, implementation of these approaches is simple: there is no ''formal'' basis, with calculations being performed directly on a real-space grid that does not depend on ion positions. The spacing of the grid is refined until the calculation converges; the grid spacing plays the role of the cutoff energy in the plane-wave approach. Secondly, since the Hamiltonian matrix is *sparse*, quadratic scaling of matrix-vector multiplication is attainable. Thirdly, there is no need to introduce artificial periodicity in dealing with nonperiodic systems. Finally, real-space methods are inherently local, which facilitates implementation on parallel computers. In short, real-space methods not only share the main advantages of plane-wave representations, but they can also have improved scaling and they can be easily parallelized, which makes them highly attractive for computation of the electronic ground states of large, complex systems.

Although one of the advantages of real-space methods is their application to localized systems, there is no reason to limit their use to such systems.[5,6] Here we present a real-space pseudopotential method for calculation of the electronic properties of *periodic* systems. Our method can be considered as an extension of the real-space method developed by our group for the study of isolated systems.[7] In Sec. II we describe the main characteristics of the new method, in Sec. III we illustrate its performance by presenting the results

of its use in a molecular-dynamics (MD) simulation of liquid silicon (as far as we know, this is the first *ab initio* MD simulation of a liquid to have employed a real-space technique), and in Sec. IV we summarize our main conclusions.

II. DESCRIPTION OF THE METHOD

According to DFT,[1,2] the total energy $E_{\rm tot}$ of a system comprising electrons and ions (the latter in positions $\{\mathbf{R}_a\}$) can be written as a unique functional of the electron density ρ,

$$E_{\rm tot}[\rho]=T[\rho]+E_{\rm ion}(\{\mathbf{R}_a\},[\rho])+E_H[\rho]+E_{\rm xc}[\rho]+E_{\rm ion\text{-}ion}(\{\mathbf{R}_a\}), \quad (1)$$

where $T[\rho]$ is the kinetic energy, $E_{\rm ion}(\mathbf{R}_a,[\rho])$ is the electron-ion energy, $E_H[\rho]$ is the electron-electron Coulomb energy or Hartree potential energy, $E_{\rm xc}[\rho]$ is the exchange-correlation energy, and $E_{\rm ion\text{-}ion}(\mathbf{R}_a)$ is the classical electrostatic energy among the ions. Finding the electron density that minimizes the energy functional is equivalent to solving the set of one-particle Schrödinger (Kohn-Sham) equations

$$\left[-\frac{\nabla^2}{2}+V_{\rm ion}(\mathbf{r})+V_H(\mathbf{r})+V_{\rm xc}(\mathbf{r})\right]\psi_n(\mathbf{r})=\epsilon_n\psi_n(\mathbf{r}) \quad (2)$$

and setting

$$\rho(\mathbf{r})=\sum_n |\psi_n(\mathbf{r})|^2, \quad (3)$$

where the sum runs over the occupied states. $V_{\rm ion}$ and V_H are the ionic and Hartree potentials, respectively; $V_{\rm xc}=\delta E_{\rm xc}/\delta\rho$. Here and in the rest of the text, we use atomic units ($e=m=\hbar=1$) unless otherwise stated. Solving Eqs. (2) and (3) requires finding a self-consistent solution for the charge density, and constitutes the most computationally intensive part of the electronic-structure calculation.

Molecular-dynamics simulations and the extraction of dynamical properties therefrom require accurate calculation of the ionic forces $\{\mathbf{F}_a\}$. If the system has been brought to the Born-Oppenheimer surface (i.e., if the single-particle wave functions are very close to the exact eigenstates), the forces can be calculated from the Hellmann-Feynman theorem,[8]

$$\mathbf{F}_a=-\frac{\partial E_{\rm tot}}{\partial \mathbf{R}_a}. \quad (4)$$

A. Solving the Kohn-Sham equations

We represent wave functions, the electron density, and potentials on a uniform orthogonal three-dimensional real-space grid. For simplicity, we assume the grid to be cubic, but the extension to a general orthorhombic grid is straightforward. In order to construct the grid, only two parameters need be specified, namely the grid spacing h (the distance between adjacent points in each of the three Cartesian directions) and the size L of the unit cell or supercell described by the cubic grid. The points of the grid are then described in a finite domain by (x_i,y_j,z_k), with the integers i, j, and k having values from 1 to $N_{\rm grid}=L/h$. The system is made periodic by replicating the unit cell and the atoms it contains (the basis) throughout space. We assume that all the atoms belong to the same species.

In order to model Eq. (2) on a real-space grid, we use a higher-order finite-difference expansion[9] for the Laplacian operator. We approximate the partial derivatives of the wave function at a given point of the grid by a weighted sum over its values at that and neighboring points.

In each iteration of the algorithm for self-consistent solution of the Kohn-Sham equations, the Hartree and exchange-correlation potentials are set up directly on the real-space grid using the approximation to the electron density obtained in the previous iteration. For $V_{\rm xc}$, we use the local-density approximation, according to which the value of $V_{\rm xc}$ at a given point is a function of the electron density at that point. To construct V_H, we solve the Poisson equation $[\nabla^2 V_H(\mathbf{r})=-4\pi\rho(\mathbf{r})]$ using the matrix formalism corresponding to the higher-order finite-difference method,[7] first setting the total charge in the supercell to zero in order to prevent the system from becoming infinitely charged due to the required periodicity.

The remaining potential term in Eq. (2), the ionic term, is determined using pseudopotential theory. We employ nonlocal norm-conserving ionic pseudopotentials cast in the Kleinman-Bylander form.[10] The ionic contribution due to one atom of the system, $V^a_{\rm ion}$, is obtained as the sum of a local term and a nonlocal term, the latter corresponding to an angular-momentum-dependent projection.[7,10] Its effect on the wave function in Eq. (2) is

$$V^a_{\rm ion}(\mathbf{r})\psi_n(\mathbf{r})=V_{\rm loc}(r_a)\psi_n(\mathbf{r})+\sum_{lm} G^a_{n,lm}u_{lm}(\mathbf{r}_a)\Delta V_l(r_a), \quad (5)$$

where $\mathbf{r}_a=\mathbf{r}-\mathbf{R}_a$; u_{lm} is the atomic pseudopotential wave function corresponding to the angular momentum quantum numbers l and m; $\Delta V_l=V_l-V_{\rm loc}$ is the difference between V_l (the l component of the ionic pseudopotential) and the local potential $V_{\rm loc}$; and the projection coefficients $G^a_{n,lm}$ given by

$$G^a_{n,lm}=\frac{1}{\langle\Delta V^a_{lm}\rangle}\int u_{lm}(\mathbf{r}_a)\Delta V_l(r_a)\psi_n(\mathbf{r})d^3r \quad (6)$$

include the normalization factor

$$\langle\Delta V^a_{lm}\rangle=\int u_{lm}(\mathbf{r}_a)\Delta V_l(r_a)u_{lm}(\mathbf{r}_a)d^3r. \quad (7)$$

The local and nonlocal terms in Eq. (5) must in principle be evaluated and accumulated for all the atoms in the system, i.e., for both the atoms in the basis and their periodic images. However, the summation of nonlocal terms is actually limited to the basis, because at distances greater than the pseudopotential core radius (a fraction of a bond length) V_l is $-Z/r$ for all l, where Z is the number of electrons acting as

valence electrons in the pseudopotential;[11] this makes ΔV_l short-ranged, so that the nonlocal terms need only be evaluated for atoms belonging to the basis. Furthermore, the integrals in Eqs. (6) and (7) can be efficiently calculated in real space by direct summation over the grid points surrounding each atom.

The situation is different for the local contribution to the ionic potential, which involves a divergent summation of the long-range Coulomb term $-Z/r$. However, this divergence can be avoided by making use of the fact that the pseudopotentials are short-ranged functions in reciprocal space.[11] The local ionic potential $V_{\mathrm{ion,loc}}$ can be calculated efficiently in reciprocal space and transferred to the real-space grid by an FFT. We obtain the local ionic potential in reciprocal space as in a plane-wave calculation with an energy cutoff of $\pi^2/2h^2$, the cutoff for which FFTs of the wave functions and potentials require a grid of size N_{grid}^3.[12] We first calculate the structure factor $S_{\mathrm{ion}}(\mathbf{q})$ at wave vector $\mathbf{q}=(2\pi/L)\times(n_x,n_y,n_z)$ (where n_x, n_y, and n_z are integers),

$$S_{\mathrm{ion}}(\mathbf{q})=\sum_a \exp(i\mathbf{q}\cdot\mathbf{R}_a), \tag{8}$$

where the sum is taken over the positions of all the atoms in a single unit cell.[13] $V_{\mathrm{ion,loc}}$ is then calculated as

$$V_{\mathrm{ion,loc}}(\mathbf{q})=S_{\mathrm{ion}}(\mathbf{q})V_{\mathrm{loc}}(q) \tag{9}$$

and transferred to the real-space grid by FFT. Note that we need to perform this transformation once, just before we enter the loop for self-consistent solution of the Kohn-Sham equations; since the local ionic potential is determined by the positions of the ions, it does not change during the process of finding a self-consistent solution for ρ.

When discretized as above, Eq. (2) adopts the form

$$\begin{aligned}-\frac{1}{2}\Bigg[&\sum_{n_1=-N}^{N} C_{n_1}\psi_n(x_i+n_1h,y_j,z_k)\\&+\sum_{n_2=-N}^{N} C_{n_2}\psi_n(x_i,y_j+n_2h,z_k)\\&+\sum_{n_3=-N}^{N} C_{n_3}\psi_n(x_i,y_j,z_k+n_3h)\Bigg]\\&+[V_{\mathrm{ion}}(x_i,y_j,z_k)+V_H(x_i,y_j,z_k)+V_{\mathrm{xc}}(x_i,y_j,z_k)]\\&\times\psi_n(x_i,y_j,z_k)=\epsilon_n\psi_n(x_i,y_j,z_k).\end{aligned} \tag{10}$$

N is the order of the finite-difference expansion. Typically, we use $N=6$. Since ΔV_l differs from zero only inside the pseudopotential core radius and the Laplacian operator extends only to a few neighbors around each grid point, the matrix representation of Eq. (10) is *very sparse*. Consequently, highly efficient diagonalization procedures can be employed to extract the required eigenvalue/eigenfunction pairs.[14,15]

B. Calculation of the forces

The total ground-state energy [Eq. (1)] is given by

$$\begin{aligned}E_{\mathrm{tot}}[\rho]=T[\rho]+\int\rho(\mathbf{r})V_{\mathrm{ion,loc}}(\mathbf{r})d^3r+\sum_{a,n,lm}\langle\Delta V_{lm}^a\rangle\\\times[G_{n,lm}^a]^2+E_H[\rho]+E_{\mathrm{xc}}[\rho]+E_{\mathrm{ion\text{-}ion}}(\{\mathbf{R}_a\})+\alpha,\end{aligned} \tag{11}$$

where the sum on n is over the occupied states and α is the contribution of the non-Coulomb part of the pseudopotential at $\mathbf{q}=\mathbf{0}$,

$$\alpha=\frac{ZN_{\mathrm{a}}^2}{L^3}\int\left(V_{\mathrm{loc}}(r)+\frac{Z}{r}\right)4\pi r^2dr. \tag{12}$$

By Eq. (4), the force on ion a is

$$\begin{aligned}\mathbf{F}_a=-\int\rho(r)\frac{\partial V_{\mathrm{loc}}(r_a)}{\partial\mathbf{R}_a}d^3r-2\sum_{n,lm}\langle\Delta V_{lm}^a\rangle G_{n,lm}^a\frac{\partial G_{n,lm}^a}{\mathbf{R}_a}\\-\frac{\partial E_{\mathrm{ion\text{-}ion}}}{\mathbf{R}_a}.\end{aligned} \tag{13}$$

The first term on the right-hand side of Eq. (13) is the contribution from the local ionic potential, $\mathbf{F}_{a,\mathrm{loc}}$. It involves the integral of a long-range function (Z/r^2), but is easily calculated in reciprocal space, where there is no long-range tail,[16]

$$\mathbf{F}_{a,\mathrm{loc}}=-iL^3\sum_{\mathbf{q}}\mathbf{q}\exp(i\mathbf{q}\cdot\mathbf{R}_a)V_{\mathrm{loc}}(q)\rho(\mathbf{q}), \tag{14}$$

where $\rho(\mathbf{q})$ is obtained by an FFT from the solution of the Kohn-Sham equations on the real-space grid. The other electronic contribution to the force is due to the nonlocal components of the pseudopotential. Taking advantage of its short range, we calculate this term in real space, in which its computation scales as the square of the system size (whereas in reciprocal space it scales as N_a^3).[17] The remaining term in Eq. (13) is the force exerted on the ion by other ions. As usual for periodic systems,[3] we evaluate this term by performing two convergent summations, one over lattice vectors and the other over reciprocal-lattice vectors, using Ewald's method.

The procedure we use to evaluate the expression given in Eq. (13) gives very accurate values of the ionic forces, as we demonstrate in Sec. III. Note that Eq. (13) contains no term representing the derivative of the basis set with respect to the position of the ion (the ''Pulay force''[18]).

III. APPLICATION TO LIQUID SILICON

As a test of our method, we performed an MD simulation of liquid silicon at a temperature of 1800 K and a density of 2.59 g/cm^3, a thermodynamic state that is close to the experimental melting point, $T_m=1680$ K, and density. This simulation constitutes a severe test because silicon is one of the most complex elemental liquids. Upon melting, silicon undergoes a transition from a semiconducting covalent struc-

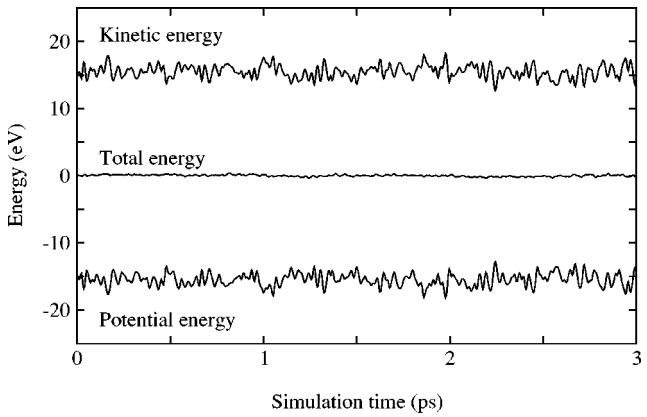

FIG. 1. Time courses of the kinetic, potential, and total energies of liquid silicon during our microcanonical real-space MD simulation. The equations of motion of the ions were integrated for a time step of 165 a.u. using the Beeman algorithm (Ref. 35). No velocity rescaling was performed. The potential and total energies have been shifted by a constant so that the total energy averages zero.

ture to a rather unusual metallic phase that, in spite of the coordination number having increased from 4 to over 6 during the transition, still has a very loosely packed structure when compared with more usual liquid metals, which have coordination numbers of about 12 (Ref. 19). The existence of covalent bonds in the metallic phase is indicative of the ''many-body'' nature of the interactions in liquid silicon, a realistic description of which requires a quantum-mechanical treatment. We compare the results of our simulation with available experimental data and with results obtained from previous MD simulations based on well-established plane-wave methods.

We considered a system of 64 atoms in a cubic supercell with $L=19.80$ a.u. The real-space grid was constructed with a spacing of $h=0.71$ a.u. The core electrons were represented by norm-conserving pseudopotentials generated for the reference configuration $[\mathrm{Ne}]3s^2 3p^2$ using the Troullier-Martins prescription,[11] with a radial cutoff of 2.5 a.u. for both *s* and *p*. The potential was made separable by the procedure of Kleinman and Bylander,[10] with the *s* potential chosen to be the local component. The local-density functional of Ceperley and Alder[20] was used as parameterized by Perdew and Zunger,[21] and the single Γ point was employed in sampling the Brillouin zone.[22]

We initially simulated the melting of solid silicon with a simple cubic structure. The temperature of the system was controlled by coupling to a virtual heat bath via a Langevin equation of motion.[23] The time step was 165 a.u. (4 fs). After the temperature had stabilized at the desired value, the system was gradually decoupled from the virtual heat bath, and a microcanonical MD simulation was performed over 750 time steps (3 ps). Only the microcanonical data were used for our analysis of the properties of liquid silicon.

A microcanonical MD run constitutes a stringent test of the accuracy of calculated ionic forces because the trajectory of the system through configuration space is deterministic. Any systematic error in the force calculations will prevent conservation of the total energy of the system. Figure 1

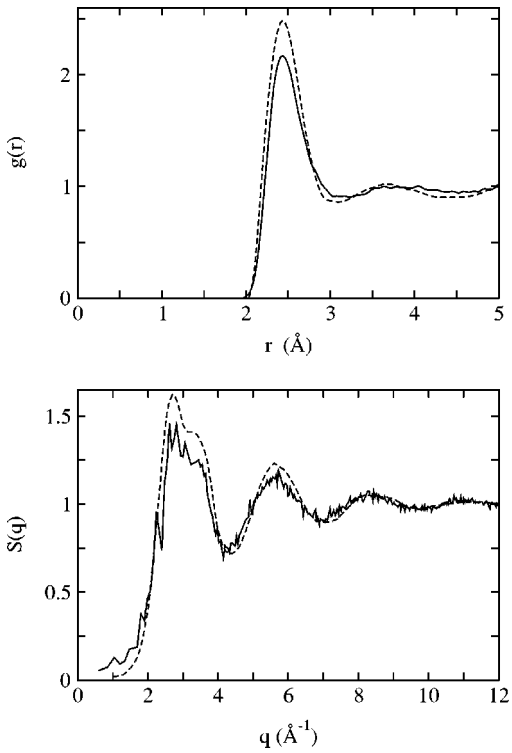

FIG. 2. Radial distribution function (upper panel) and static structure factor (lower panel) of liquid silicon. The continuous curves represent our real-space MD results, the dashed curves experimental data from Ref. 26.

shows that there is no such error in our simulation. The kinetic and potential energies perform bounded oscillations around stable mean values, and the oscillations of one almost cancel those of the other, resulting in very good conservation of the total energy. The rms noise in the energy conservation is less than 0.003 eV/at. No drift in the total energy was observed. Highly accurate forces imply more than the validity of the scheme used in their calculation (Sec. II B). Since errors in the Hellmann-Feynman forces are first-order with respect to errors in the wave functions, accurate forces can only be obtained when the wave functions are very nearly exact eigenstates, which implies that the procedure used to discretize and solve the Kohn-Sham equations (Sec. II A) is also very accurate.

It should be noted that we were able to use relatively long time steps in integrating the equations of motion. This is a characteristic of *ab initio* MD methods that restrict the simulation to the Born-Oppenheimer surface (BOMD). The philosophy is different in the Car-Parrinello method (CPMD).[24] In CPMD, the construction of a fully self-consistent field at each time step is avoided by using fictitious dynamics for the electrons, but accurate integration of the equations of motion requires the use of time steps more than an order of magnitude smaller than those employed in BOMD.

Figure 2 shows results on the static structure[25] of liquid silicon obtained from the simulation and by experiment.[26] The two sets of data for the radial distribution function $g(r)$ agree well (upper panel); the simulation results give the correct position of the principal peak of the function, 2.43 Å,

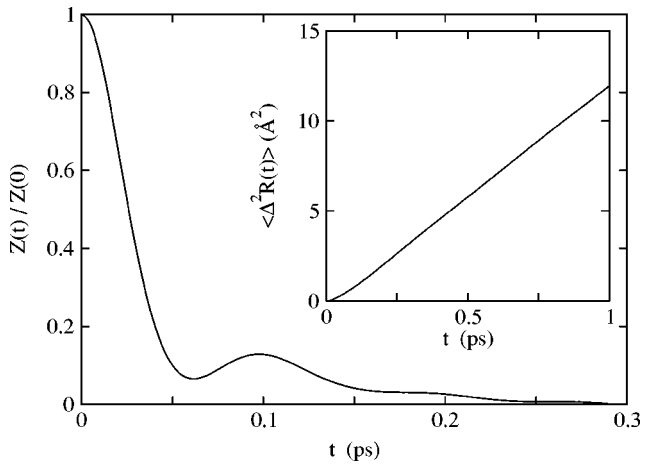

FIG. 3. Normalized velocity autocorrelation function $Z(t)/Z(0)$ and mean-square displacement $\langle \Delta R^2(t) \rangle$ (inset) of liquid silicon as obtained from our real-space MD simulation.

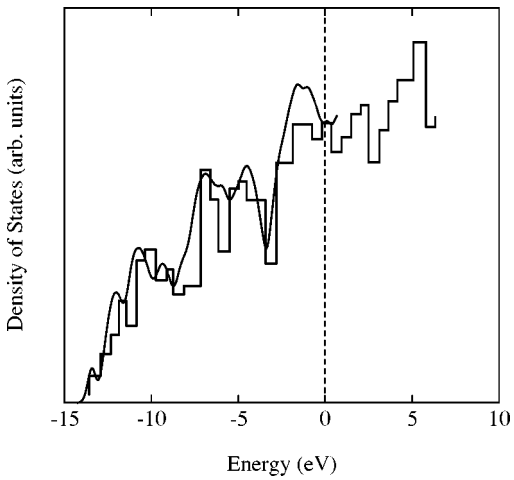

FIG. 4. Electronic density of states of liquid silicon as obtained from our real-space MD simulation. The histogram is from a previous plane-wave MD simulation (Ref. 33). Fermi levels are set to zero.

and exhibit the correct trend at greater distances (though without dispersion). Integrating $g(r)$ up to the position of the first minimum determined by experiment, 3.10 Å, affords a value for the average coordination number that is identical to experimental estimates, ~ 6.4 (Ref. 26).

Comparison between the results of simulation and experiment for the static structure factor $S(q)$ (Fig. 2, lower panel) is a stronger test than comparison of $g(r)$ results because it is $S(q)$ that is obtained directly from experimental measurements. $g(r)$ is obtained by Fourier transform of $S(q)$, and is more susceptible to numerical errors. $S(q)$ was calculated from the simulation results using the expression[25]

$$S(q) = \frac{1}{N_a} \left\langle \sum_i \sum_j \exp[-i\mathbf{q}\cdot(\mathbf{R}_i - \mathbf{R}_j)] \right\rangle, \qquad (15)$$

where the sums are taken over the ions in the unit cell and the angular brackets denote averaging over both the trajectories of the particles during the microcanonical MD run and over all the wave vectors $\mathbf{q}$ with the same modulus q (we assume that liquid silicon is macroscopically isotropic). In terms of $S(q)$, the agreement between simulation and experiment is very good, the simulation results correctly predicting all the successive maxima and minima of the function. Note, in particular, the successful prediction of the shoulder to the right of the first peak, which is not shown by the $S(q)$ functions of simple liquid metals.[27,28]

As examples of time-dependent functions, we calculated the mean-square displacement, $\langle \Delta R^2(t) \rangle$, and the velocity autocorrelation function $Z(t)$ (Fig. 3).[25] Except for very small values of t, $\langle \Delta R^2(t) \rangle$ is perfectly linear, in keeping with the theoretical expression[25]

$$\langle \Delta R^2(t) \rangle \sim 6Dt + c \quad \text{as} \quad t \to \infty, \qquad (16)$$

in which D is the self-diffusion coefficient and c is a constant. $Z(t)$ tends to zero with increasing time due to the absence of correlation between the velocity of each particle and its initial value. It is interesting that $Z(t)$ does not take negative values; this contrasts with the typical behavior of simple liquid metals, which near the melting point, exhibit the so-called ''cage effect'' [the atoms surrounding any given atom allow the latter to move over short distances but then reflect it, causing $Z(t)$ to change sign].[29,30] The absence of such backscattering in liquid silicon is likely related to its small average coordination number.

Like $\langle \Delta R^2(t) \rangle$, the velocity autocorrelation function is related to the self-diffusion coefficient,[25]

$$D = \int_0^\infty Z(t)dt. \qquad (17)$$

The values of D obtained from our simulation data via Eqs. (16) and (17) are both the same, 2.1 Å ^{2}/ps. This value is consistent with those afforded by previous *ab initio* calculations using plane-wave representations: BOMD results for $\langle \Delta R^2(t) \rangle$ have given a value of $D = 1.9$ Å ^{2}/ps,[31,32] and a CPMD study has yielded values of 2.3 Å ^{2}/ps [from $\langle \Delta R^2(t) \rangle$] and 2.0 Å ^{2}/ps [from $Z(t)$].[33] A simulation based on interatomic potentials gave $D = 1.0$ Å ^{2}/ps,[34] a value significantly smaller than the quantum-mechanical estimates.

Figure 4 shows the electronic density-of-states distribution for liquid silicon. This distribution was obtained by constructing a histogram of the eigenvalues every 10 time steps during the microcanonical MD run and averaging these results. For comparison, the density of states obtained in an earlier CPMD study[33] of the same thermodynamic state is also shown (both studies only considered the Kohn-Sham states at the single Γ point). The agreement between the two approaches is quite good, bearing in mind the technical differences between BOMD and CPMD calculations. Both studies clearly show liquid silicon to be a good metal with a large density of states at the Fermi level.

IV. SUMMARY AND CONCLUSIONS

This paper presents a method for self-consistent *ab initio* calculation of electronic structures of periodic systems. Our

method employs pseudopotentials to construct the electron--ion potential, and solves the Kohn-Sham equations on a uniform real-space grid. The only FFT performed is used to set up the local ionic potential on the real-space grid following its calculation in reciprocal space. The efficiency deriving from inherent parallelizability and the use of sparse matrices makes this method eminently suitable for the study of large complex systems. Calculation of the forces on ions has also been implemented.

We have successfully tested the accuracy of the method by performing an MD simulation of liquid silicon and comparing the results with available experimental data and with previous *ab initio* results. To the best of our knowledge, this simulation constitutes the first application of an *ab initio* real-space technique to the study of a liquid, and proves the ability of these approaches to simulate the liquid state.

ACKNOWLEDGMENTS

We would like to thank J.L. Martins and E. Lorin for helpful discussions. We would like to acknowledge support from the National Science Foundation and the United States Department of Energy. Computational support was provided by the National Energy Research Scientific Computing Center and the Minnesota Supercomputing Institute. This work was supported in part by the Army High Performance Computing Research Center (AHPCRC) under the auspices of the Department of Army, Army Research Laboratory (ARL) under Cooperative Agreement number DAAD19-01-2-0014, the content of which does not necessarily reflect the position or the policy of the government; no official endorsement should be inferred. L.K. acknowledges the generous support of the Estelle Funk foundation and the Delta Career Development Center.

[1] P. Hohenberg and W. Kohn, Phys. Rev. B **136**, B864 (1964).
[2] W. Kohn and L. J. Sham, Phys. Rev. A **140**, A1133 (1965).
[3] See, for example, W. E. Pickett, Comput. Phys. Rep. **9**, 115 (1989); M. C. Payne, M. P. Teter, D. C. Allan, T. A. Arias, and J. D. Joannopoulos, Rev. Mod. Phys. **64**, 1045 (1992).
[4] See, for example, T. L. Beck, Rev. Mod. Phys. **72**, 1041 (2000).
[5] E. L. Briggs, D. J. Sullivan, and J. Bernholc, Phys. Rev. B **54**, 14 362 (1996).
[6] N. A. Modine, G. Zumbach, and E. Kaxiras, Phys. Rev. B **55**, 10 289 (1997).
[7] J. R. Chelikowsky, N. Troullier, and Y. Saad, Phys. Rev. Lett. **72**, 1240 (1994); J. R. Chelikowsky, N. Troullier, K. Wu, and Y. Saad, Phys. Rev. B **50**, 11 355 (1994).
[8] H. Hellmann, *Einführung in die Quantumchemie* (Deuticke, Leipzig, 1937); R. P. Feynman, Phys. Rev. **56**, 340 (1939).
[9] G. D. Smith, *Numerical Solutions of Partial Differential Equations: Finite Difference Methods*, 2nd ed. (Oxford University Press, New York, 1978).
[10] L. Kleinman and D. M. Bylander, Phys. Rev. Lett. **48**, 1425 (1982).
[11] N. Troullier and J. L. Martins, Phys. Rev. B **43**, 1993 (1991).
[12] J. L. Martins and M. L. Cohen, Phys. Rev. B **37**, 6134 (1988).
[13] The inclusion of a periodic image of an atom in the summation on the right-hand side of Eq. (8) would give the same contribution as that of the atom, since their exponential terms would differ by $2\pi n$, with n an integer.
[14] Y. Saad, *Iterative Methods of Sparse Linear Systems* (PWS, Boston, 1996).
[15] R. Lehoucq, D.C. Sorensen, and C. Yang, *Arpack User's Guide: Solution of Large-Scale Eigenvalue Problems With Implicitly Restarted Arnoldi Methods* (SIAM, Philadelphia, 1998).
[16] J. Ihm, A. Zunger, and M. L. Cohen, J. Phys. C **12**, 4409 (1979).
[17] R. D. King-Smith, M. C. Payne, and J. S. Lin, Phys. Rev. B **44**, 13 063 (1991).
[18] P. Pulay, Mol. Phys. **17**, 197 (1969).
[19] T. E. Faber, *Introduction to the Theory of Liquid Metals* (Cambridge University Press, Cambridge, England, 1972).
[20] D. M. Ceperley and B. J. Alder, Phys. Rev. Lett. **45**, 566 (1980).
[21] J. P. Perdew and A. Zunger, Phys. Rev. B **23**, 5048 (1981).
[22] In Sec. II it was implicitly assumed that Brillouin-zone sampling would be restricted to the Γ point, but generalization of Eq. (2) to an arbitrary Bloch wave vector would not raise fundamental new points in the discussion of its discretization (see Ref. 5).
[23] N. Binggeli, J. L. Martins, and J. R. Chelikowsky, Phys. Rev. Lett. **68**, 2956 (1992).
[24] R. Car and M. Parrinello, Phys. Rev. Lett. **55**, 2471 (1985).
[25] J. P. Hansen and I. R. McDonald, *Theory of Simple Liquids* (Academic, London, 1986).
[26] Y. Waseda and K. Suzuki, Z. Phys. B: Condens. Matter **20**, 339 (1975).
[27] W. Jank and J. Hafner, Phys. Rev. B **41**, 1497 (1990); **42**, 6926 (1990); **42**, 11 530 (1990).
[28] M. M. G. Alemany, O. Diéguez, C. Rey, and L. J. Gallego, Phys. Rev. B **60**, 9208 (1999).
[29] U. Balucani, A. Torcini, and R. Vallauri, Phys. Rev. A **46**, 2159 (1992).
[30] M. M. G. Alemany, C. Rey, and L. J. Gallego, Phys. Rev. B **58**, 685 (1998).
[31] J. R. Chelikowsky and N. Binggeli, Solid State Commun. **88**, 381 (1993).
[32] V. Godlevsky, J. R. Chelikowsky, and N. Troullier, Phys. Rev. B **52**, 13 281 (1995).
[33] I. Štich, R. Car, and M. Parrinello, Phys. Rev. Lett. **63**, 2240 (1989); I. Štich, R. Car, and M. Parrinello, Phys. Rev. B **44**, 4262 (1991).
[34] P. B. Allen and J. Q. Broughton, J. Phys. Chem. **91**, 4964 (1987).
[35] D. Beeman, J. Comput. Phys. **20**, 130 (1976).